DNA Damage, Poly(ADP-Ribose) Polymerase Activation, and Phosphorylated Histone H2AX Expression During Postnatal Retina Development in C57BL/6 Mouse

David Martín-Oliva,[1] Sandra M. Martín-Guerrero,[1] Ana M. Matia-González,[2] Rosa M. Ferrer-Martín,[1] María Martín-Estebané,[1] María-Carmen Carrasco,[1] Ana Sierra,[1] José L. Marín-Teva,[1] Ruth Calvente,[1] Julio Navascués,[1] and Miguel A. Cuadros[1]

[1]Departamento de Biología Celular, Facultad de Ciencias, Universidad de Granada, Granada, Spain
[2]Department of Microbial and Cellular Sciences, Faculty of Health and Medical Sciences (FHMS), University of Surrey, Guildford, United Kingdom

Correspondence: David Martín-Oliva, Departamento de Biología Celular, Facultad de Ciencias, Universidad de Granada, E-18071 Granada, Spain; dmoliva@ugr.es.

Submitted: October 8, 2014
Accepted: January 22, 2015

Citation: Martín-Oliva D, Martín-Guerrero SM, Matia-González AM, et al. DNA damage, poly(ADP-ribose) polymerase activation, and phosphorylated histone H2AX expression during postnatal retina development in C57BL/6 mouse. *Invest Ophthalmol Vis Sci*. 2015;56:1301–1309. DOI:10.1167/iovs.14-15828

Purpose. The purpose of this study was to investigate the incidence of DNA damage during postnatal development of the retina and the relationship between DNA damage and cell death.

Methods. DNA damage in the developing postnatal retina of C57BL/6 mice was assessed by determining the amounts of 8-hydroxy-2′-deoxyguanosine (8-OHdG), which is indicative of DNA oxidation and related to the formation of DNA single-strand breaks (SSBs), and phosphorylated histone H2AX (γ-H2AX), a marker of DNA double-strand breaks (DSBs). Poly(ADP-ribose) polymerase (PARP) activation was measured by ELISA and Western blotting. The location of γ-H2AX–positive and dying cells was determined by immunofluorescence and TUNEL assays.

Results. Oxidative DNA damage was maintained at low levels during high PARP activation between postnatal days 0 (P0) and P7. Phosphorylated histone H2AX gradually increased between P0 and P14 and decreased thereafter. Phosphorylated histone H2AX–positive cells with cell death morphology or TUNEL positivity were more abundant at P7 than at P14.

Conclusions. Oxidative DNA damage in postnatal retina increases during development. It is low during the first postnatal week when PARP-1 activity is high but increases thereafter. The rise in DSBs when PARP activity is downregulated may be attributable to accumulated oxidative damage and SSBs. At P7 and P14, γ-H2AX–positive cells are repairing naturally occurring DNA damage, but some are dying (mostly at P7), probably due to an accumulation of irreparable DNA damage.

Keywords: DNA damage, γ-H2AX, PARP-1, postnatal development, retina

A consequence of the high rate of oxygen consumption in the retina[1] is the generation of reactive oxygen species (ROS), including free radicals, peroxides, and singlet oxygen atoms.[2] Reactive oxygen species harm cells by oxidizing proteins, lipids, and DNA. ROS production is neutralized in part by antioxidant molecules and by enzymes such as the mitochondrial enzyme manganese superoxide dismutase (MnSOD), which converts two molecules of superoxide anions into water and hydrogen peroxide.[3] Oxidative stress, therefore, can be considered an imbalance between the production of oxidative molecules and the antioxidant capacity of the cell.

Oxidative DNA damage derives from the attack of free radicals against deoxyribose and usually affects only one of the two strands of DNA molecules (single-strand breaks [SSBs]). Single-strand breaks can also appear during base excision repair (BER), which is the usual mechanism for repairing oxidative DNA damage.[4,5] Single-strand breaks that are not successfully repaired may originate double-strand breaks (DSBs),[6,7] the most deleterious type of DNA damage, because a single unrepaired DSB is sufficient to induce cell death. Double-strand breaks are repaired by recombination mechanisms (homologous or nonhomologous end-joining) other than those involved in BER.[4] Double-strand breaks can result from the action of external factors (e.g., X-rays or chemical agents) but are also produced during normal tissue development and differentiation.[8,9]

Poly(ADP-ribose) polymerase (PARP) enzymes catalyze the polymerization of ADP-ribose units (PAR polymer) from donor NAD^+ molecules on target proteins.[10] PARP-1 is the founding member of the PARP family and is responsible for approximately 85% to 90% of PAR polymer formation in the cell.[11,12] In most eukaryotes, BER and SSBs are initially detected by PARP-1, which binds to DNA strand breaks and induces the poly(ADP) ribosylation of proteins that participate in DNA repair, including itself.[13,14] Consequently, PARP-1 activation is increased under pathophysiological conditions that affect DNA[15,16] in the brain[17] and retina,[18,19] among others. Given our previous finding that PARP-1 expression and activity are upregulated in the mouse retina during the first week of normal postnatal development,[20] most of the PARP activity observed in the developing retina is likely attributable to PARP-1 activation.

Table. Sources and Dilutions of the Primary Antibodies Used for Immunoblotting

Antibody	Sources and References	Dilution
Mouse monoclonal anti-MnSOD	Catalog no. sc-133134; Santa Cruz Biotechnology, Dallas, TX, USA	1:5000
Mouse monoclonal anti-PAR	Catalog no. ALX-804-220; Alexis Biochemicals, San Diego, CA, USA	1:400
Rabbit monoclonal anti-γH2AX	Catalog no. NB100-79967; Novus Biologicals, Cambridge, UK	1:5000
Rabbit polyclonal anti-3-NT	Catalog no. 06-284; Millipore, Billerica, MA, USA	1:500
Rabbit polyclonal anti-β tubulin	Catalog no. T2200; Sigma-Aldrich Corp., St. Louis, MO, USA	1:10000

Reactive oxygen species are produced during neural development, because the developing neurons require high rates of transcription and translation, associated with increased endogenous metabolism and mitochondrial activity, in order to achieve their differentiation. In the present study, we demonstrated that oxidative DNA damage increases during postnatal development of the retina. Oxidative damage is maintained at low levels during early postnatal development, whereas PARP activity is upregulated but increases when this activity becomes downregulated. Downregulation of PARP is also accompanied by a transient increase in phosphorylated histone H2AX (γ-H2AX), an early marker of DSBs.[21,22]

Materials and Methods

Animals

C57BL/6 mice were provided by the Animal Experimentation Service of the University of Granada (Granada, Spain) and maintained in a 12-hour light:12-hour dark cycle with access to food and water ad libitum. Early postnatal (P) animals were killed by decapitation and older ones by cervical dislocation. Retinas were dissected from newborn (P0), 3-day-old (P3), P7, P14, P21, and P60 (adult) animals. All experimental procedures followed guidelines issued by the Animal Experimentation Ethics Committee of the University of Granada (permit 2011-357) and adhered to the Association for Research in Vision and Ophthalmology Statement on the Use of Animals in Ophthalmic and Vision Research.

8-Hydroxy-2′-Deoxyguanosine Detection by ELISA

Oxidative DNA stress was measured with an ELISA kit for quantitative detection of the oxidative DNA adduct 8-hydroxy-2′-deoxyguanosine (8-OHdG, new 8-OHdG check kit; JaICA, Shizuoka, Japan). Cell lysates from the retinas were homogenized with a Dounce homogenizer (Afora, Madrid, Spain) in 1 mL DNAzol reagent (Life Technologies, Gaithersburg, MD, USA), centrifuged at 9800*g* for 10 minutes at 4°C, and precipitated in 0.5 mL 100% ethanol. DNA was then washed with 75% ethanol and resuspended in 8 mM NaOH. Finally, DNA was quantified using a BioPhotometer Plus (Eppendorf, Hamburg, Germany), and 10 μg DNA from each sample was digested by DNase I (Sigma-Aldrich Corp., St. Louis, MO, USA) for 15 minutes at room temperature and loaded in triplicate into 96-well plates. Finally, absorbance at 450 nm of the ELISA reaction was determined in a Multiskan Ascent reader (Thermo Fisher Scientific, Rockford, IL, USA). Three different retinas were analyzed at each age.

Determination of PARP Activity by ELISA

PARP activity was measured with the HT Colorimetric PARP/apoptosis assay (Trevigen, Gaithersburg, MD, USA). Cell lysates from retinas of animals at P0, P7, P14, P21, and P60 were obtained according to the manufacturer's protocol. Part of the supernatant served to quantify the concentration of proteins by Bradford's method (Protein Assay; Bio-Rad, Hercules, CA, USA), whereas 200 ng proteins from each sample was analyzed with the ELISA kit following the manufacturer's instructions. The absorbance of this reaction, which correlates with PARP enzyme activity, was measured using a Multiskan Ascent reader (Thermo Fisher Scientific). Samples from three different retinas were analyzed in triplicate at each age.

Western Blot Analysis

Protein extracts from both retinas of the same animal were used, following a previously described procedure.[20] After protein quantification (Bio-Rad protein assay), 35 μg proteins was loaded into each well of an SDS-polyacrylamide gel and run in a mini-gel system (Bio-Rad); the proteins were transferred onto polyvinylidene fluoride membrane (Immun-Blot; Bio-Rad) and incubated overnight in primary antibody. Detection of MnSOD, PAR, γ-H2AX, 3-nitrotyrosine, and β-tubulin by Western blot (WB) was carried out by using the primary antibodies and dilutions listed in the Table.

After blocking with phosphate-buffered saline (PBS) containing 5% milk powder and 0.1% Tween-20, blots were incubated for 2 hours with the corresponding secondary antibody (peroxidase-conjugated anti-mouse immunoglobulin G [IgG] or peroxidase-conjugated anti-rabbit IgG; both from Sigma-Aldrich Corp.).

Antibody reaction was documented with ChemiDoc-It imaging system (UVP, Cambridge, UK) using a chemiluminescence reagent (Immobilon Western chemiluminescent horseradish-peroxidase substrate; Merck KGaA, Darmstadt, Germany). Densitometric analyses were carried out using ChemiDoc-It imaging system software (UVP). The level of protein expression was normalized relative to the expression level of β-tubulin.

Immunocytochemistry and TUNEL Assay

Enucleated eyes from P7 and P14 pups were fixed in periodate-lysine-paraformaldehyde[23] for 6 hours at 4°C, cryoprotected in PBS with 20% sucrose, and frozen in liquid nitrogen; 20-μm–thick cross-sections were blocked with 5% normal goat serum (NGS; Sigma-Aldrich Corp.) in PBS for 1 hour. and incubated overnight at 4°C with the same anti-γ-H2AX antibody as for WB (diluted 1:200 in 0.1% NGS-PBS). After being washed, samples were incubated for 2 hours at room temperature in secondary antibody (Alexa fluor 488-conjugated goat anti-rabbit IgG or Alexa fluor 594-conjugated goat anti-rabbit IgG [both from Molecular Probes, Eugene, OR, USA]) diluted 1:1000 in 0.1% NGS-PBS. Finally, nuclei were counterstained with Hoechst 33342 (Sigma-Aldrich Corp.), washed in PBS, and mounted with Fluoromount G (Southern Biotech, Birmingham, AL, USA). The primary antibody was omitted from some sections as negative controls.

Several sections were double-labeled for the detection of γ-H2AX by immunohistochemistry and cell death by the TUNEL technique. First, immunodetection of γ-H2AX was performed as described above, followed by incubation in 2% terminal

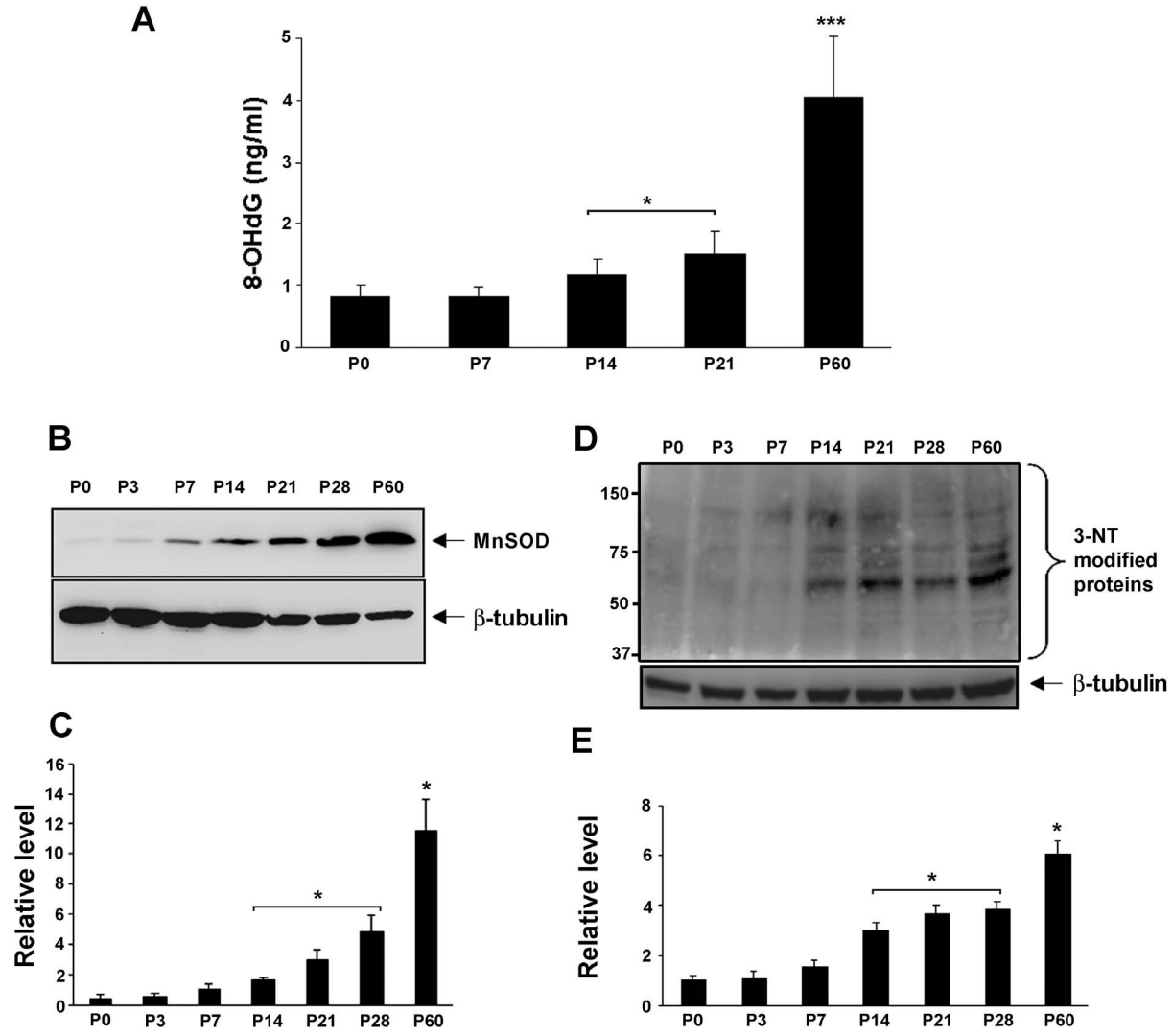

FIGURE 1. Oxidative damage in the postnatal mouse retina. (**A**) ELISA assay shows that 8-OHdG, a marker of oxidative DNA damage, began to increase significantly from P14 on. $n = 3$ at all ages. *Significant differences ($P < 0.05$) between the marked values and P0 to P7; ***significant differences ($P < 0.001$) between P60 and the remaining values. (**B**) Immunoblots ($n = 3$) of MnSOD reveal that expression of this enzyme in the retina increased progressively during development. Beta-tubulin was used as the loading control. (**C**) Densitometric analysis of MnSOD ($n = 3$) shows relative levels of increased values of this enzyme during postnatal retina development. *Significant differences ($P < 0.05$) between the marked values and the preceding ones. (**D**) Immunoblots ($n = 4$) of 3-NT show different bands corresponding to the oxidation-modified proteins by ROS in the postnatal retina. Beta-tubulin was used as the loading control. (**E**) Densitometric analysis of 3-NT ($n = 4$). Note that this oxidative modification increased from P14 on, as in (**A**). *Significant differences ($P < 0.05$) between the marked values and the preceding ones.

deoxynucleotidyl transferase (TDT) enzyme (Promega, Madison, WI, USA) in TDT buffer (Promega) and 0.03% fluorescein-deoxyuridine triphosphate nucleotides (dUTP; Roche Diagnostics, Indianapolis, IN, USA) for 1 hour at 37°C. After incubation, sections were washed with PBS and stained with the nuclear dye Hoechst 33342.

Confocal images were obtained with a TCS-SP5 microscope (Leica, Wetzlar, Germany) or A1R confocal microscope (Nikon GmbH, Dusseldorf, Germany). Images were stored in tagged image file format and digitally prepared in Photoshop (Adobe Systems, San Jose, CA, USA) to adjust the brightness and contrast.

TUNEL-positive cells with or without γ-H2AX immunostaining were recorded in all layers of five high-power fields (5 HPF) per section of P7 and P14 retinas (three retinas per age and three sections per retina), using a fluorescence microscope (Axiophot; Zeiss, Oberkochen, Germany) with a 40× objective (original magnification ×400). Results were expressed as percentage of TUNEL-labeled cells with or without γ-H2AX immunostaining.

Statistical Analysis

Quantitative data were expressed as means ± SEM from at least three independent experiments for each age. Statistical significance was determined by using the Student *t*-test.

RESULTS

Oxidative DNA Damage

Results of 8-OHdG ELISA revealed that oxidative damage was low in the developing retina at P0 and remained at comparable levels during the first postnatal week. However, 8-OHdG significantly increased during the second week of postnatal development, and a major increase was observed in adult retinas (Fig. 1A).

Increased oxidative damage may be indicated by the presence of mechanisms that prevent it. We tested this possibility by

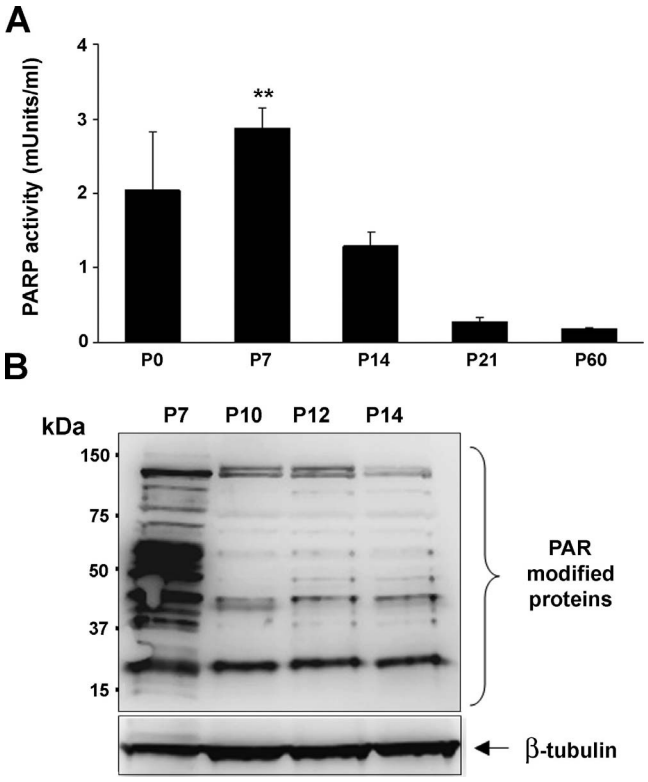

FIGURE 2. Activity of PARP, a BER protein, during retinal development. (**A**) PARP activity, as measured by ELISA, increased during the first week of postnatal development of the retina and decreased thereafter. **Significant differences ($P < 0,01$) between P7 and subsequent values. (**B**) Immunoblot of poly(ADP) ribosylated proteins (representative of three immunoblots) show that, in accordance with results shown in (**A**), the amount of poly(ADP) ribosylated proteins produced by PARP activity significantly decreased after P7. Beta-tubulin was used as the loading control.

determining retinal expression during postnatal development of MnSOD, an enzyme involved in elimination of ROS and contribution to increasing the longevity of retinal cells.[24] The WB results revealed a progressive increase in the amount of MnSOD protein during development (Figs. 1B, 1C), paralleling the increase observed in DNA oxidative damage. Increased expression of the MnSOD protein appears to be related to the oxidative damage, as it is absent when the damage is very low and increases with greater damage. However, the increased oxidative damage observed in the retina does not appear to be prevented by this augmented expression of MnSOD.

In order to verify that ROS increased throughout postnatal development despite the increased expression of MnSOD, we assessed the presence of 3-nitrotyrosine (3-NT)-modified proteins in the retina. It has been reported that the production of 3-NT proteins depends on the level of oxidative damage and therefore gives an indication of its severity.[25] Western blot data demonstrated that the level of 3-NT in mouse postnatal retina was significantly upregulated during development (Figs. 1D, 1E). This result is consistent with the above-reported increase in oxidative DNA damage in the retina.

Activation of PARP-1, a BER Protein

Base excision repair processes, the main oxidative DNA damage repair pathway, were determined by studying the activation in postnatal retina of PARP-1, responsible for more than 85% of PARP activity. PARP-1 plays a critical role in sensing

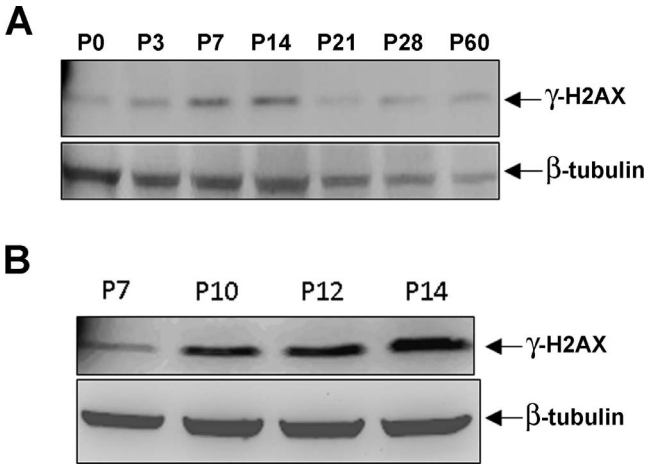

FIGURE 3. Expression of γ-H2AX during development of the retina. (**A**) Immunoblots of postnatal retinal lysates incubated with an antibody reveal the phosphorylation of Ser-139 in H2AX (γ-H2AX), which gradually increased from P0 to P14 and decreased thereafter. The highest increase in γ-H2AX was observed at P14, coinciding with the absence of PARP-1 expression.[20] Western blot is representative of three experiments. (**B**) Detailed analysis of γ-H2AX expression during the second postnatal week of development shows that this expression markedly increased between P7 and P14. Immunoblots were repeated three times. Beta-tubulin was used as the loading control.

this DNA damage and initiating repair.[14,26–28] ELISA results showed that PARP activity was higher during the first week of postnatal retina development and decreased thereafter, whereas low PARP activity was found in the adult retina (Fig. 2A). The WB study also detected abundant PAR-modified proteins at P7, with a marked reduction after this age (Fig. 2B). These concordant ELISA and WB results are also in agreement with previously reported findings.[20]

The above data suggest that the effectiveness of the retinal BER pathway is high during the first postnatal week of development but greatly reduced thereafter. Thus, oxidative DNA damage is kept at low levels until P7 but then increases after a reduction in PARP activity. This increase is not prevented by antioxidant enzymes such as MnSOD.

γ-H2AX, a DSB Marker: Expression and Distribution

Immunoblots of postnatal retinal lysates showed that γ-H2AX gradually increased from P0 to P14 and decreased thereafter (Fig. 3A). More detailed analysis of the second week of postnatal development (Fig. 3B) confirmed that the highest increase in γ-H2AX was at P14, when PARP-1 expression and activity began to decrease (Fig. 2; also see Fig. 3 in Ref. 20).

The distribution of γ-H2AX immunopositive cells was determined by immunohistochemical staining at the end of the first (P7), second (P14), and third weeks (P21) of postnatal retinal development (Fig. 4A). Phosphorylated histone H2AX immunostaining was detected mostly in the prospective inner nuclear layer (INL) and ganglion cell layer (GCL) of P7 and P14 retinas (Fig. 4A, upper panels), although immunostained cells were more abundant at P14 than at P7. The robust immunostaining at P14 contrasted with the lesser staining found at P21 in the same regions (Fig. 4A, bottom left panel). These immunohistochemical observations are in accordance with the WB results, as can be observed by comparing them with the WB densitometry data (Fig. 4B). The graph in Figure 4B shows that γ-H2AX expression was 1.9- and 5.2-fold higher at P14 than at P7 and P21, respectively.

Investigative Ophthalmology & Visual Science

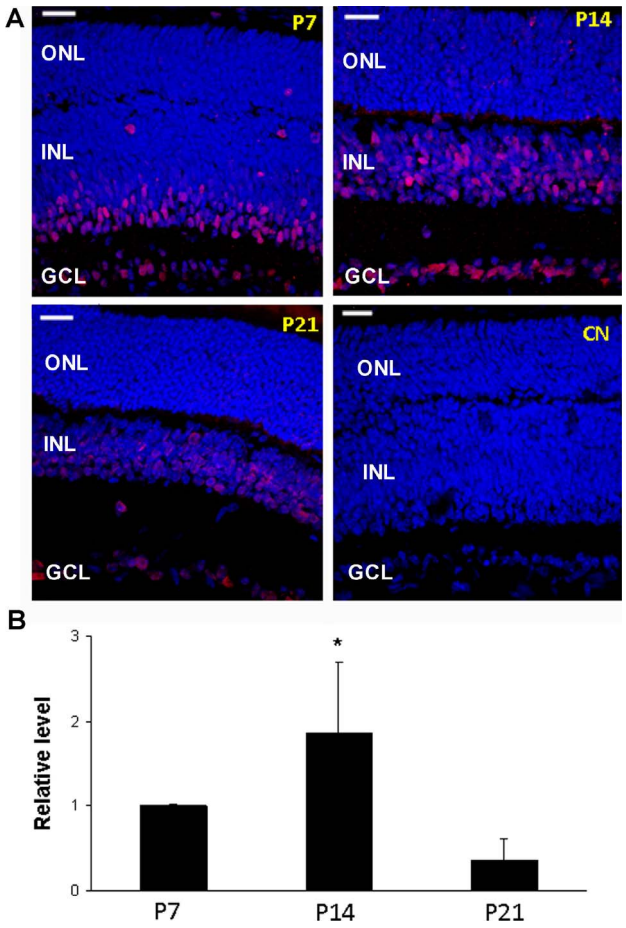

FIGURE 4. Distribution and quantification of γ-H2AX expression between P7 and P21. (**A**) Confocal microscopy shows immunocytochemical labeling of γ-H2AX (*red*) and Hoechst staining (*blue*) of the retinal layers. Nearly all labeled cells at P7 are in the prospective inner nuclear layer (INL) and ganglion cell layer (GCL); this observation agreed with observations performed at P14, when γ-H2AX immunolabeling appears mostly in the INL and GCL. However, weaker immunolabeling was seen at P21 in the same regions. CN, control section in which the primary antibody was not applied; ONL, outer nuclear layer. *Scale bars*: 20 μm. (**B**) Densitometric analysis of γ-H2AX from three immunoblots (one of them appears in Fig. 3A) of extracts obtained from retinas on P7, P14, and P21. *Significant differences ($P < 0.05$) between P7 and P21 values.

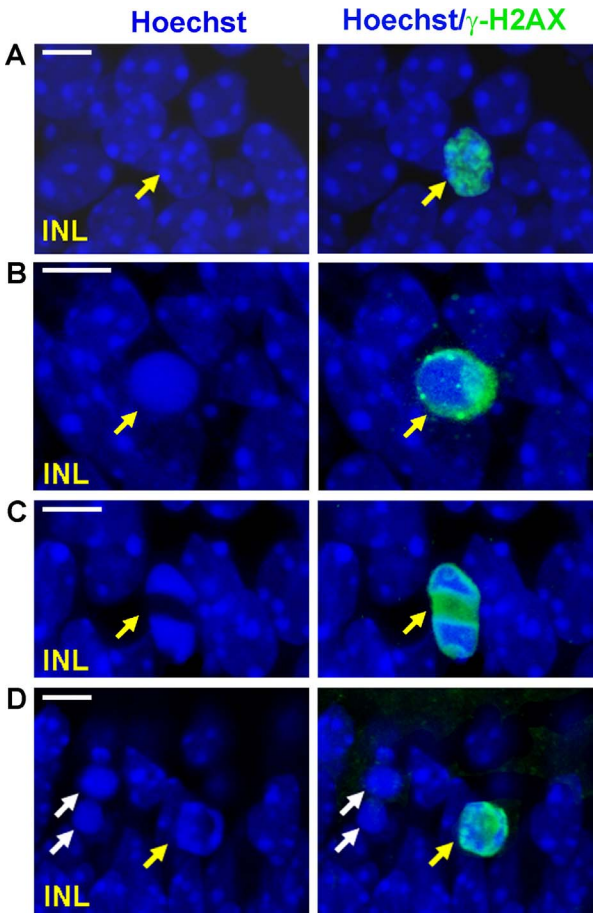

FIGURE 5. Confocal photomicrographs show γ-H2AX immunolabeling in P7 retinas. All images were taken in the inner nuclear layer (INL) and are representative of findings obtained in at least three different retinas. Hoechst staining (*blue*) of the chromatin is illustrated in the *left column* and is shown with the γ-H2AX immunolabeling (*green*) in the *right column* (**A**). Phosphorylated histone H2AX distribution in a nucleus that appears normal, which is likely undergoing DNA repair (*yellow arrow*). (**B**) A pyknotic nucleus (*yellow arrow*) also shows γ-H2AX immunolabeling. (**C**) A nucleus with two clumps of intensely stained chromatin (*yellow arrow*) shows that γ-H2AX immunolabeling was excluded from the regions containing condensed chromatin. (**D**) A nucleus with clear signs of degeneration is γ-H2AX–positive (*yellow arrow*), whereas two pyknotic nuclei (*white arrows*) are devoid of immunolabeling. *Scale bars*: 5 μm.

Colocalization of γ-H2AX With Dying Cells in Postnatal Retinal Cells

Some features of γ-H2AX-labeled cells differed between P7 and P14 retinas. At P7, most of them had nuclei with normal chromatin distribution, as revealed by Hoechst staining (Fig. 5A), but other immunopositive nuclei showed clear signs of degeneration, with large clumps of condensed chromatin and pyknosis (Figs. 5B, 5C, left panels). The strong γ-H2AX immunoreactivity of these cells was circumscribed to nuclear areas not occupied by condensed chromatin (Figs. 5B, 5C, right panels). Frequently, nuclei showing morphological signs of cell death lacked any γ-H2AX immunostaining, despite being in close proximity to γ-H2AX-labeled nuclei (Fig. 5D). In contrast, the γ-H2AX immunostaining seen at P14 was habitually restricted to apparently normal nuclei, detected by Hoechst staining, in both the GCL (Fig. 6A) and the INL (Fig. 6B), and it therefore appeared to be related to DNA repair rather than cell degeneration.

Sections from P7 and P14 retinas were double-labeled for γ-H2AX immunostaining and TUNEL technique to clarify the distribution of labeled cells (Fig. 7). The microscope images showed that TUNEL-positive cells were more abundant in retinas at P7 than at P14 (15.9 TUNEL-positive nuclei/5 HPF at P7 versus 5.9/5 HPF at P14 [see Materials and Methods]), and the localization of cell death in the nuclear layers changed from INL at P7 to outer nuclear layer (ONL) at P14, as previously reported.[29]

A large fraction (74.0%) of TUNEL-positive cells showed immunoreactivity for γ-H2AX in P7 retinas (Figs. 8A, 8B); however, only 31.5% of TUNEL-positive cells were also immunoreactive for γ-H2AX in P14 retinas (Figs. 8C, 8D).

Taken together, these results suggest that a large number of γ-H2AX–positive retinal cells are repairing DNA damage at P7 and at P14. Nevertheless, a proportion of them are dying, mostly at P7, possibly due to an accumulation of irreparable DNA damage.

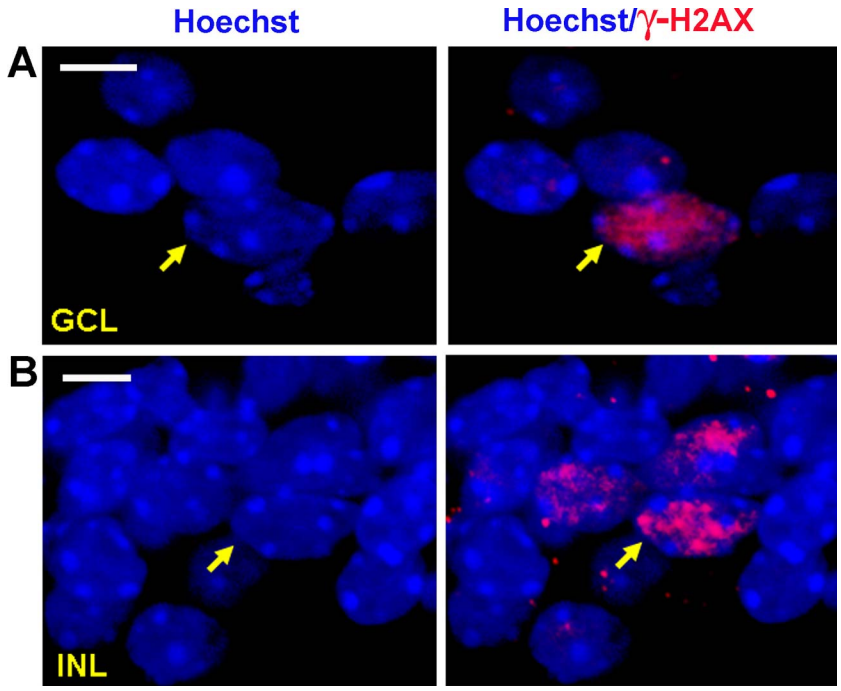

FIGURE 6. Confocal images show the appearance of γ-H2AX immunolabeling in the ganglion cell layer (GCL) and inner nuclear layer (INL) of P14 retinas. Observations were made in three retinas from each age. Images at *left* show the nuclear morphology as revealed by Hoechst staining (*blue*), whereas those at *right* exhibit the Hoechst and γ-H2AX immunolabeling (*red*) together. Labeled nuclei (*yellow arrows*) have a normal appearance in both the GCL (**A**) and INL (**B**). *Scale bars*: 2 μm.

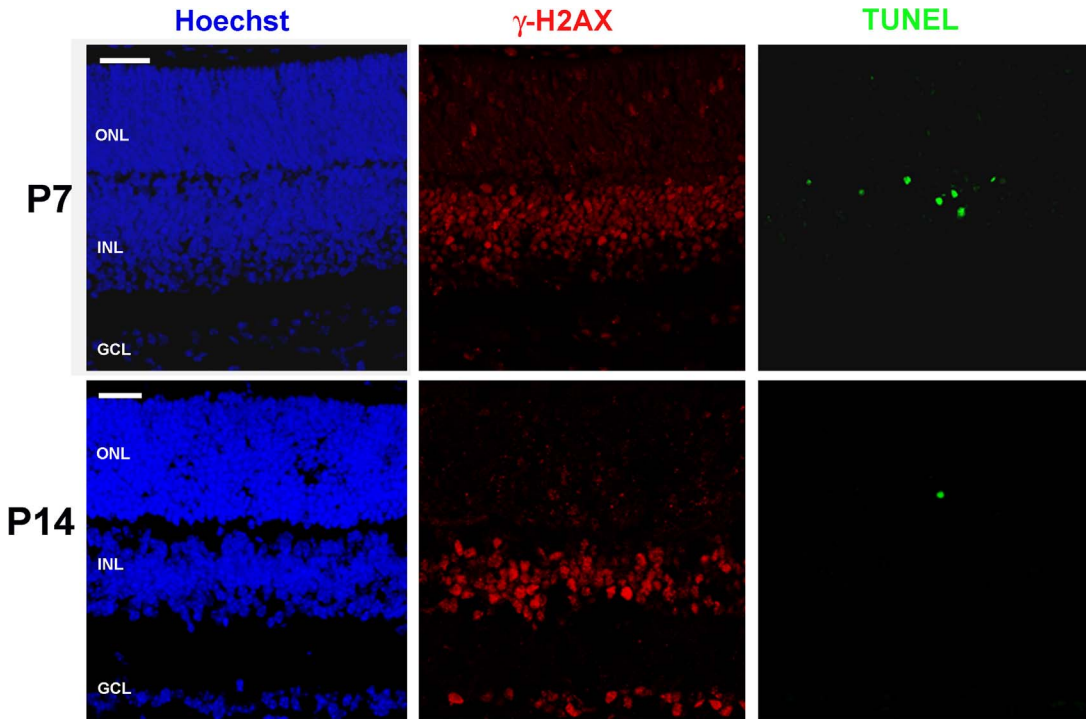

FIGURE 7. Distribution of γ-H2AX immunolabeling (*red, central column*) and TUNEL-positive nuclei (*green, right column*) in P7 and P14 retinas. Hoechst staining (*blue, left column*) was used to reveal the retinal layers. At P7, TUNEL-positive nuclei were more abundant than at P14 and were localized mainly in the inner nuclear layer (INL) and frequently in nuclei with γ-H2AX immunostaining. However, labeled cells in the P14 retinas are found in regions with weak or no γ-H2AX immunolabeling. *Scale bars*: 30 μm.

Investigative Ophthalmology & Visual Science

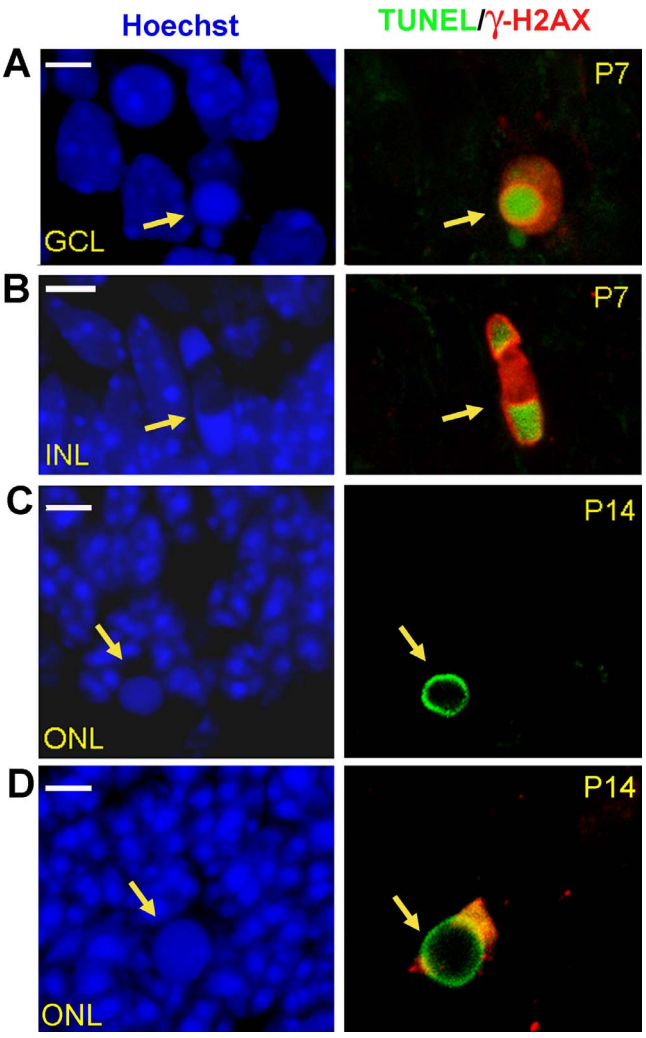

Figure 8. High-magnification images (original magnification ×600) of TUNEL staining and γ-H2AX immunostaining in P7 and P14 retinas. *Left column*: Chromatin pattern of apparently degenerating cells (arrows [Hoechst staining, *blue*]); *right column*: TUNEL staining (*green*) and γ-H2AX immunolabeling (*red*) of the same cells. (**A**) Pyknotic nucleus (*arrow*) in the ganglion cell layer (GCL) of a P7 retina stained by TUNEL and showing γ-H2AX immunoreactivity. (**B**) Phosphorylated histone H2AX–positive nucleus with two clumps of chromatin (*arrow*) that is also TUNEL-labeled; note that immunostaining appears in the region of noncondensed chromatin in the inner nuclear layer (INL) of a P7 retina. (**C**) Pyknotic nucleus (*arrow*) within the outer nuclear layer (ONL) of a P14 retina; the nucleus is labeled by TUNEL but does not show detectable γ-H2AX immunostaining. (**D**) Detail of a pyknotic TUNEL-positive nucleus in the same layer (*arrow*) at P14 that is also γ-H2AX–positive. *Scale bars*: 5 μm (**A**, **B**); 3 μm (**C**); 3.5 μm (**D**).

Discussion

We investigated the time course of oxidative DNA damage in developing retina under physiological conditions and analyzed its relationship with two proteins, PARP-1 and γ-H2AX, sensors of DNA damage. DNA damage may produce cell death, which is a relatively frequent event during development of the retina, as reported by Péquignot et al.[29] and Young.[30] Both of those studies found, using different techniques, that cell death levels are higher during the first week of postnatal development of the mouse retina and decrease during the second postnatal week, in agreement with a previous report by our group.[20]

Oxidative DNA Damage in Postnatal Retina

Oxidative DNA damage was low during the first week of development but increased thereafter. During the second postnatal week, the retina was exposed to new situations, and its cells were stimulated by external light for the first time at approximately P14, when the eyes open. A relationship between these new conditions and the increase in DNA damage cannot be ruled out.

A study of γ-H2AX labeling in embryonic and early postnatal (P2) mouse neuroretinas reported the presence of DSBs during retinal development.[31] The authors attributed this damage to oxidative stress, replication stress, or transcriptional activity during early development. Our study extends their observations by revealing that DNA damage increases with older age.

It has been claimed that the accumulation of damage during life is responsible for the deterioration of cell components and aging.[32,33] Oxidative stress and DNA damage in the retina have been related to the progression of age-related macular degeneration, diabetic retinopathy, and inherited retinal degenerations.[34–36] A possible factor in the pathogenesis of these retinal diseases is the contribution of oxidative stress to cell death via DNA damage and the stimulation of apoptotic pathways.[37,38]

Various antioxidants have proven useful to delay the development of retinal diseases,[39,40] including MnSOD, whose upregulation protects against oxidative damage in the diabetic retina.[24,41,42] Mitochondrial enzyme manganese superoxide dismutase expression increased in the retina after P7 but so did the oxidative DNA damage, indicating that the upregulation of MnSOD is not sufficient to prevent the oxidative damage. The hydrogen peroxide generated by MnSOD activity, together with the decrease in catalase enzyme activity that has been observed in the developing retina,[43] may promote the release of ROS via the Fenton reaction.[44] Therefore, many ROS are not eliminated during normal development, perhaps because they are needed for the normal development and maturation of the retina, as postulated in other regions of the central nervous system.[45,46]

DNA Damage and PARP-1 Activation

Activation of PARP-1 is observed during the repair of SSBs and DSBs.[14] PARP-1 recognizes the sites of DNA strand breaks and recruits and activates proteins involved in their subsequent repair.[27,28,47] Hence, the decrease in PARP activity reported here likely results in a reduction in this repair capacity. This is more clearly the case for BER, in which the involvement of PARP activity is better understood.[14,28] Consequently, the increased PARP activation levels during the first week of postnatal retina development likely ameliorate oxidative DNA damage through more effective DNA repair, as described in other models.[48] The reduction in PARP activity and BER is unlikely to be the sole explanation of increased cell damage after the first postnatal week, when other factors may play a role (e.g., electrical activity and exposure to light). It is worth noting that the oxidative DNA damage increased once the PARP activity decreased.

Some authors have reported that excessive poly(ADP) ribosylation may contribute to cell death in the pathological retina, because PARP-1 upregulation may trigger cell death instead of DNA repair.[18,19,49,50] Hence, PARP-1 activity may either prevent cell death or promote it. In fact, it appears that a mild activation of PARP-1, such as that observed under physiological conditions, would result in DNA repair, whereas an intense or excessive activation would induce cell death.[11,17,51]

Investigative Ophthalmology & Visual Science

Different Responses to DNA Damage During Postnatal Retina Development

Our study suggests that DNA repair capability changes during the development of the retina. This is consistent with reports stating that proliferating cells are equipped with complete and active DNA repair pathways that are partially downregulated in terminally differentiated cells.[52,53] Interestingly, the decrease in PARP activity coincides with the appearance of markers of the differentiation of specific retinal types and with the formation of the ONL,[54] which begins to establish the definitive retinal layers. Therefore, the data suggest that BER mechanisms are downregulated, at least partially, when cell differentiation becomes predominant in the retina.

Downregulation of some components of cell death pathways has also been described at similar times during retinal development.[55–58] It therefore appears that repair and cell death mechanisms both diminish when the retina matures.

DSBs in the Postnatal Retina

Phosphorylated histone H2AX increased from birth to the end of the second week of postnatal development but markedly decreased during the third postnatal week. This increase may be related to the final differentiation process of numerous retinal cells at these times. It has been reported that DSBs result from the restructuring of chromatin that takes place during differentiation.[59,60] In fact, γ-H2AX decreases at P21, when most retinal cells are already differentiated and synaptogenesis is well under way.[61,62]

Many γ-H2AX-labeled nuclei appear to be repairing DNA damage at P7 and P14, and some were associated with cell death in a larger proportion at P7 than at P14, in agreement with previous reports of no direct relationship between cell death and γ-H2AX in the embryonic mouse retina.[31] Given that cell death continues to be observed at P14, although greatly diminished (see Fig. 1 in Ref. 20), it can be concluded that different cell death pathways are present in the postnatal retina: one that is related to DSB production (i.e., γ-H2AX–positive) and one that is not. Further studies are required to identify the factors that determine the death pathway followed by a given cell.

In summary, we report that oxidative DNA damage accumulates during development of the postnatal retina, apparently in relationship with the downregulation of certain DNA damage repair mechanisms. Further research is necessary to establish whether these downregulated mechanisms are replaced by others during postnatal retina development of the mouse retina.

Acknowledgments

The authors thank David Porcel and Ana M. Santos (CIC, University of Granada) for assistance with confocal microscopy.

Supported by Ministerio de Economía y Competitividad, Spain, Grant BFU2010-19981, Junta de Andalucía, Spain, Grant P07-CVI-03008, and University of Granada, Spain, Grant GREIB PYR_2011_19. The funding organizations did not participate in the design, execution of the experimental work, or writing of this report. The authors alone are responsible for the content and writing of the paper.

Disclosure: **D. Martín-Oliva**, None; **S.M. Martín-Guerrero**, None; **A.M. Matia-González**, None; **R.M. Ferrer-Martín**, None; **M. Martín-Estebané**, None; **M.-C. Carrasco**, None; **A. Sierra**, None; **J.L. Marín-Teva**, None; **R. Calvente**, None; **J. Navascués**, None; **M.A. Cuadros**, None

References

1. Trick GL, Berkowitz BA. Retinal oxygenation response and retinopathy. *Prog Retin Eye Res*. 2005;24:259–274.
2. Jones DP. Radical-free biology of oxidative stress. *Am J Physiol Cell Physiol*. 2008;295:C849–C868.
3. Thannickal VJ, Fanburg BL. Reactive oxygen species in cell signaling. *Am J Physiol Lung Cell Mol Physiol*. 2000;279:L1005–L1028.
4. Polo SE, Jackson SP. Dynamics of DNA damage response proteins at DNA breaks: a focus on protein modifications. *Genes Dev*. 2011;25:409–433.
5. Robertson AB, Klungland A, Rognes T, Leiros I. DNA repair in mammalian cells: Base excision repair: the long and short of it. *Cell Mol Life Sci*. 2009;66:981–993.
6. Cadet J, Douki T, Gasparutto D, Ravanat JL. Oxidative damage to DNA: formation, measurement and biochemical features. *Mutat Res*. 2003;531:5–23.
7. Rassool FV, Gaymes TJ, Omidvar N, et al. Reactive oxygen species, DNA damage, and error-prone repair: a model for genomic instability with progression in myeloid leukemia? *Cancer Res*. 2007;67:8762–8771.
8. Jackson SP. Sensing and repairing DNA double-strand breaks. *Carcinogenesis*. 2002;23:687–696.
9. Vilenchik MM, Knudson AG. Endogenous DNA double-strand breaks: production, fidelity of repair, and induction of cancer. *Proc Natl Acad Sci U S A*. 2003;100:12871–12876.
10. Ame JC, Spenlehauer C, de Murcia G. The PARP superfamily. *Bioessays*. 2004;26:882–893.
11. Virag L, Szabo C. The therapeutic potential of poly(ADP-ribose) polymerase inhibitors. *Pharmacol Rev*. 2002;54:375–429.
12. Aguilar-Quesada R, Munoz-Gamez JA, Martin-Oliva D, et al. Modulation of transcription by PARP-1: consequences in carcinogenesis and inflammation. *Curr Med Chem*. 2007;14:1179–1187.
13. Burkle A. Physiology and pathophysiology of poly(ADP-ribosyl)ation. *Bioessays*. 2001;23:795–806.
14. De Vos M, Schreiber V, Dantzer F. The diverse roles and clinical relevance of PARPs in DNA damage repair: current state of the art. *Biochem Pharmacol*. 2012;84:137–146.
15. Szabo C. DNA strand breakage and activation of poly-ADP ribosyltransferase: a cytotoxic pathway triggered by peroxynitrite. *Free Radic Biol Med*. 1996;21:855–869.
16. Szabo C, Virag L, Cuzzocrea S, et al. Protection against peroxynitrite-induced fibroblast injury and arthritis development by inhibition of poly(ADP-ribose) synthase. *Proc Natl Acad Sci U S A*. 1998;95:3867–3872.
17. Kauppinen TM, Swanson RA. The role of poly(ADP-ribose) polymerase-1 in CNS disease. *Neuroscience*. 2007;145:1267–1272.
18. Li GY, Osborne NN. Oxidative-induced apoptosis to an immortalized ganglion cell line is caspase independent but involves the activation of poly(ADP-ribose) polymerase and apoptosis-inducing factor. *Brain Res*. 2008;1188:35–43.
19. Paquet-Durand F, Silva J, Talukdar T, et al. Excessive activation of poly(ADP-ribose) polymerase contributes to inherited photoreceptor degeneration in the retinal degeneration 1 mouse. *J Neurosci*. 2007;27:10311–10319.
20. Martin-Oliva D, Ferrer-Martin RM, Santos AM, et al. Simultaneous cell death and upregulation of poly(ADP-ribose) polymerase-1 expression in early postnatal mouse retina. *Invest Ophthalmol Vis Sci*. 2011;52:7445–7454.
21. Rogakou EP, Pilch DR, Orr AH, Ivanova VS, Bonner WM. DNA double-stranded breaks induce histone H2AX phosphorylation on serine 139. *J Biol Chem*. 1998;273:5858–5868.

Investigative Ophthalmology & Visual Science

22. Yuan J, Adamski R, Chen J. Focus on histone variant H2AX: to be or not to be. *FEBS Lett*. 2010;584:3717–3724.
23. Yamato S, Hirabayashi Y, Sugihara H. An improved procedure for the histochemical demonstration of cathepsin D by the mercury-labeled pepstatin method. *Stain Technol*. 1984;59: 113–120.
24. Kanwar M, Chan PS, Kern TS, Kowluru RA. Oxidative damage in the retinal mitochondria of diabetic mice: possible protection by superoxide dismutase. *Invest Ophthalmol Vis Sci*. 2007;48:3805–3811.
25. Buddi R, Lin B, Atilano SR, et al. Evidence of oxidative stress in human corneal diseases. *J Histochem Cytochem*. 2002;50: 341–351.
26. Srivastava DK, Berg BJ, Prasad R, et al. Mammalian abasic site base excision repair. Identification of the reaction sequence and rate-determining steps. *J Biol Chem*. 1998;273:21203–21209.
27. de Murcia JM, Niedergang C, Trucco C, et al. Requirement of poly(ADP-ribose) polymerase in recovery from DNA damage in mice and in cells. *Proc Natl Acad Sci U S A*. 1997;94:7303–7307.
28. Dantzer F, de La Rubia G, Menissier-De Murcia J, Hostomsky Z, de Murcia G, Schreiber V. Base excision repair is impaired in mammalian cells lacking poly(ADP-ribose) polymerase-1. *Biochemistry*. 2000;39:7559–7569.
29. Péquignot MO, Provost AC, Sallé S, et al. Major role of BAX in apoptosis during retinal development and in establishment of a functional postnatal retina. *Dev Dyn*. 2003;228:231–238.
30. Young RW. Cell death during differentiation of the retina in the mouse. *J Comp Neurol*. 1984;229:362–373.
31. Baleriola J, Suarez T, de la Rosa EJ. DNA-PK promotes the survival of young neurons in the embryonic mouse retina. *Cell Death Differ*. 2010;17:1697–1706.
32. Hamilton ML, Van Remmen H, Drake JA, et al. Does oxidative damage to DNA increase with age? *Proc Natl Acad Sci U S A*. 2001;98:10469–10474.
33. Ishii N. Oxidative stress and aging in Caenorhabditis elegans. *Free Radic Res*. 2000;33:857–864.
34. Beatty S, Koh H, Phil M, Henson D, Boulton M. The role of oxidative stress in the pathogenesis of age-related macular degeneration. *Surv Ophthalmol*. 2000;45:115–134.
35. Kowluru RA, Koppolu P, Chakrabarti S, Chen S. Diabetes-induced activation of nuclear transcriptional factor in the retina, and its inhibition by antioxidants. *Free Radic Res*. 2003; 37:1169–1180.
36. Komeima K, Rogers BS, Lu L, Campochiaro PA. Antioxidants reduce cone cell death in a model of retinitis pigmentosa. *Proc Natl Acad Sci U S A*. 2006;103:11300–11305.
37. Carmody RJ, Cotter TG. Oxidative stress induces caspase-independent retinal apoptosis in vitro. *Cell Death Differ*. 2000; 7:282–291.
38. Sanvicens N, Gomez-Vicente V, Masip I, Messeguer A, Cotter TG. Oxidative stress-induced apoptosis in retinal photoreceptor cells is mediated by calpains and caspases and blocked by the oxygen radical scavenger CR-6. *J Biol Chem*. 2004;279: 39268–39278.
39. O'Driscoll C, Doonan F, Sanvicens N, Messeguer A, Cotter TG. A novel free radical scavenger rescues retinal cells in vivo. *Exp Eye Res*. 2011;93:65–74.
40. Payne AJ, Kaja S, Naumchuk Y, Kunjukunju N, Koulen P. Antioxidant drug therapy approaches for neuroprotection in chronic diseases of the retina. *Int J Mol Sci*. 2014;15:1865–1886.
41. Kowluru RA, Kowluru V, Xiong Y, Ho YS. Overexpression of mitochondrial superoxide dismutase in mice protects the retina from diabetes-induced oxidative stress. *Free Radic Biol Med*. 2006;41:1191–1196.
42. Kowluru RA, Atasi L, Ho YS. Role of mitochondrial superoxide dismutase in the development of diabetic retinopathy. *Invest Ophthalmol Vis Sci*. 2006;47:1594–1599.
43. Liles MR, Newsome DA, Oliver PD. Antioxidant enzymes in the aging human retinal pigment epithelium. *Arch Ophthalmol*. 1991;109:1285–1288.
44. Loh A, Hadziahmetovic M, Dunaief JL. Iron homeostasis and eye disease. *Biochim Biophys Acta*. 2009;1790:637–649.
45. Massaad CA, Klann E. Reactive oxygen species in the regulation of synaptic plasticity and memory. *Antioxid Redox Signal*. 2011;14:2013–2054.
46. Sunico CR, Portillo F, Gonzalez-Forero D, Moreno-Lopez B. Nitric-oxide-directed synaptic remodeling in the adult mammal CNS. *J Neurosci*. 2005;25:1448–1458.
47. Trucco C, Oliver FJ, de Murcia G, Menissier-de Murcia J. DNA repair defect in poly(ADP-ribose) polymerase-deficient cell lines. *Nucleic Acids Res*. 1998;26:2644–2649.
48. Swindall AF, Stanley JA, Yang ES. PARP-1: friend or foe of DNA damage and repair in tumorigenesis? *Cancers (Basel)*. 2013;5: 943–958.
49. Weise J, Isenmann S, Bahr M. Increased expression and activation of poly(ADP-ribose) polymerase (PARP) contribute to retinal ganglion cell death following rat optic nerve transection. *Cell Death Differ*. 2001;8:801–807.
50. Obrosova IG, Julius UA. Role for poly(ADP-ribose) polymerase activation in diabetic nephropathy, neuropathy and retinopathy. *Curr Vasc Pharmacol*. 2005;3:267–283.
51. Kauppinen TM, Swanson SH. Poly(ADP-ribose) polymerase is a mediator of necrotic cell death by ATP depletion. *Proc Natl Acad Sci U S A*. 1999;96:13978–13982.
52. Fortini P, Ferretti C, Dogliotti E. The response to DNA damage during differentiation: pathways and consequences. *Mutat Res*. 2013;743–744:160–168.
53. Barzilai A, Biton S, Shiloh Y. The role of the DNA damage response in neuronal development, organization and maintenance. *DNA Repair (Amst)*. 2008;7:1010–1027.
54. Sharma RK, O'Leary TE, Fields CM, Johnson DA. Development of the outer retina in the mouse. *Brain Res Dev Brain Res*. 2003;145:93–105.
55. Donovan M, Cotter TG. Caspase-independent photoreceptor apoptosis in vivo and differential expression of apoptotic protease activating factor-1 and caspase-3 during retinal development. *Cell Death Differ*. 2002;9:1220–1231.
56. Donovan M, Doonan F, Cotter TG. Decreased expression of pro-apoptotic Bcl-2 family members during retinal development and differential sensitivity to cell death. *Dev Biol*. 2006; 291:154–169.
57. Madden SD, Donovan M, Cotter TG. Key apoptosis regulating proteins are down-regulated during postnatal tissue development. *Int J Dev Biol*. 2007;51:415–423.
58. O'Driscoll C, Donovan M, Cotter TG. Analysis of apoptotic and survival mediators in the early post-natal and mature retina. *Exp Eye Res*. 2006;83:1482–1492.
59. Falk M, Lukasova E, Kozubek S. Higher-order chromatin structure in DSB induction, repair and misrepair. *Mutat Res*. 2010;704:88–100.
60. Falk M, Lukasova E, Stefancikova L, et al. Heterochromatinization associated with cell differentiation as a model to study DNA double strand break induction and repair in the context of higher-order chromatin structure. *Appl Radiat Isot*. 2014; 83Pt B;177–185.
61. Tian N. Developmental mechanisms that regulate retinal ganglion cell dendritic morphology. *Dev Neurobiol*. 2011;71: 1297–1309.
62. Xu H, Tian N. Pathway-specific maturation, visual deprivation, and development of retinal pathway. *Neuroscientist*. 2004;10: 337–346.

Investigative Ophthalmology & Visual Science